Landscape Ecol (2013) 28:271–283
DOI 10.1007/s10980-012-9833-1

RESEARCH ARTICLE

Landscape configuration and urban heat island effects: assessing the relationship between landscape characteristics and land surface temperature in Phoenix, Arizona

John Patrick Connors · Christopher S. Galletti · Winston T. L. Chow

Received: 16 July 2012 / Accepted: 5 December 2012 / Published online: 19 December 2012

Abstract The structure of urban environments is known to alter local climate, in part due to changes in land cover. A growing subset of research focuses specifically on the UHI in terms of land surface temperature by using data from remote sensing platforms. Past research has established a clear relationship between land surface temperature and the proportional area of land covers, but less research has specifically examined the effects of the spatial patterns of these covers. This research considers the rapidly growing City of Phoenix, Arizona in the United States. To better understand how landscape structure affects local climate, we explored the relationship between land surface temperature and spatial pattern for three different land uses: mesic residential, xeric residential, and industrial/commercial. We used high-resolution (2.4 m) land cover data and an ASTER temperature product to examine 90 randomly selected sample sites of 240 square-meters. We (1) quantify several landscape-level and class-level landscape metrics for the sample sites, (2) measure the Pearson correlation coefficients between land surface temperature and each landscape metric, (3) conduct an analysis of variance among the three land uses, and (4) model the determinants of land surface temperature using ordinary least squares linear regression. The Pearson's correlation coefficients reveal significant relationships between several measures of spatial configuration and LST, but these relationships differ among the land uses. The ANOVA confirmed that mean land surface temperature and spatial patterns differed among the three land uses. Although a relationship was apparent between surface temperatures and spatial pattern, the results of the linear regression indicate that proportional land cover of grass and impervious surfaces alone best explains temperature in mesic residential areas. In contrast, temperatures in industrial/commercial areas are explained by changes in the configuration of grass and impervious surfaces.

Keywords ASTER · Quickbird · Remote sensing · CAP-LTER · Urban temperature

J. P. Connors (✉)
EcoSERVICES Group, Arizona State University, P.O. Box 875302, Tempe, AZ 85287-5302, USA
e-mail: johnpconnors@asu.edu

J. P. Connors · C. S. Galletti
School of Geographical Sciences and Urban Planning, Arizona State University, P.O. Box 875302, Tempe, AZ 85287-5302, USA

W. T. L. Chow
Department of Engineering, Arizona State University, 7231 E Sonoran Arroyo Mall, 330 Santan Hall, Mesa, AZ 85212, USA

Introduction

Impervious surfaces and built structures in urban areas alter local climate through the urban heat island (UHI) (Oke 1987; Quattrochi and Ridd 1994), whose impacts

can have regional-scale consequences (Kalnay and Cai 2003). The UHI refers to the relatively higher surface and air temperatures that occur in urban areas as a result of land cover changes and waste energy arising from urbanization (Oke 1995). UHIs are generally best observed at night, as rates of urban cooling are slower than cooling over "rural" or natural surfaces, due to greater urban thermal inertia, i.e. slower release of stored energy from the urban surface (Oke 1987). Intra-urban variations in temperatures are a significant feature arising from the UHI, and largely result from modifications to (i) urban structure (e.g. height-to-width ratio of buildings and streets); (ii) urban cover (e.g. proportion of built-up vs. vegetated surfaces per unit area); (iii) urban fabric (e.g. physical properties of concrete, asphalt etc.); and (iv) urban metabolism (e.g. waste energy from human activities; Oke 2004). Apart from affecting UHI intensity (i.e. the difference in magnitude between urban–rural temperatures), the cumulative effects of these changes reduce the variance between daytime and nighttime temperatures (Quattrochi et al. 2000). Growing urban populations and urban sprawl probably exacerbates the UHI effect through feedbacks implicit in the urbanization process. For instance, conversion of rural surfaces to concrete or asphalt increases surface heat storage and decreases nocturnal urban cooling. The ensuing warmer temperatures likely results in greater air-conditioning demand, thus increasing energy use and latent mechanical heat output (Landsberg 1981).

In general, the effects of the UHI have implications for the ecological footprints of urban areas and on human wellbeing. Heat stress, for example, poses a health hazard as temperatures rise and normal physiological processes can no longer regulate body temperature, as evidenced by increased hospitalizations and emergency calls during heat waves (Kalkstein and Smoyer 1993; Kinney et al. 2001). Vulnerability to heat stress depends upon a population's sensitivity to physical exposure to local environmental conditions and its adaptive capacity, such as access to air conditioning; the latter presents an environmental justice issue whereby lower income urban residents face greater risk of heat stress (Klinenberg 2002; Harlan et al. 2006). Residential landscaping may exacerbate disparities in heat exposure, as lower income communities generally have less vegetation compared to wealthier neighborhoods (Chow et al. 2012). Along with the hazard of heat stress, the UHI also affects the diurnal concentration and vertical mixing of several urban pollutants that detrimentally affect respiratory health, e.g. ground-level ozone (Lee et al. 2003). Furthermore, increased UHI intensities may threaten the sustainability of water supplies in already water-stressed regions as urban residents demand more water for outdoor use (Gober et al. 2011), particularly for irrigation of non-native vegetation. Increased water usage, however, also serves as a method to mitigate high urban temperatures through evapotranspiration (Goward et al. 1985; Gober 2006).

General investigation of the UHI is mostly focused on canopy-layer temperatures, which includes the atmosphere between the urban surface and mean building height (Oke 2004), but a notable research subset concentrates on the surface UHI phenomenon, utilizing land surface temperature (LST) data obtained from remote sensing platforms (e.g. Nichol 1996; Zhang et al. 2009; Jin 2012), and its relation to urban surface physical characteristics (Voogt and Oke 2003). Within this theme, the urban cover, or spatial composition in the city landscape (i.e. the relative amounts of the component land cover types, such as forest cover or concrete surfaces; Gustafson 1998), is important in determining intra-urban UHI intensities (Rosenzweig et al. 2005; Zhou et al. 2011). For example, greater proportions of urban green-spaces reduce surface temperatures relative to areas largely consisting of manmade materials like concrete and asphalt (Jenerette et al. 2007). Less well known is the impact of urban structure, or spatial configuration, i.e. the spatial arrangement and structural characteristics of land cover patches within a city (Gustafson 1998). Though this latter topic is less explored, emerging research suggests that land architecture—encompassing the kind, magnitude and pattern of land uses and covers (Turner 2010)—may significantly influence surface UHI, especially at micro ($\sim$100 m^2) to local ($\sim$1 km^2) scales.

In examining the meteorological and climatological influence of spatial configuration on surface UHI morphology, a pertinent approach would be to adopt techniques from related scientific disciplines. The field of landscape ecology has long-been concerned with measuring spatial configuration, and has developed metrics to quantify the spatial characteristics of land cover patches and their relationships to one another (McGarigal and Marks 1995; Turner et al. 2001). Despite the pervasiveness of these methods for

applications in other disciplines, few surface UHI studies have employed these to examine the relationship between configuration and LST. A possible reason for the lack of prior study of urban spatial configuration was due to restricted data availability, as fine resolution data are required for detailed urban land-cover mapping. Although coarse and medium resolution data (e.g. Landsat and MODIS) are readily available, pixels often span multiple land covers and create problems of mixed pixels in heterogeneous urban areas (e.g. Small 2005). Thermal data generally have coarser spatial resolution than shorter wavelength bands, placing further limitations on UHI studies. For example, the resolution of Landsat TM's and ASTER's thermal bands are 60 and 90 m respectively, despite both having resolutions of 30 and 15 m for other bands. Several LST studies have emphasized the relationship between landscape composition/urban cover with temperatures without directly considering spatial configuration/urban structure (e.g. Voogt and Oke 2003; Weng 2003; Jenerette et al. 2007; Buyantuyev and Wu 2010), though some recent works have considered size and shape of vegetation patches as factors influencing urban LST. For example, Zhang et al. (2009) used Landsat ETM + data to derive urban LST from Nanjing, China, and noted that the spatial characteristics and configurations of vegetation patches within cities have varied impacts on the distribution of LST. Cao et al. (2010) also analyzed ASTER data from park spaces in Nagoya, Japan, and found that park shape influences temperatures.

Increasing availability of fine resolution data (e.g. Quickbird at 2.4 m) and advanced image analysis methods, however, are supporting urban land cover mapping and UHI studies. For example, through ASTER imagery taken over Indianapolis, U.S.A., Weng et al. (2008) found an interesting relationship between LST in residential areas and its spatial configuration, with more complex residential zonal polygons resulting in greater variations of LST. In the same city, Liu and Weng (2009) analyzed the influence of scaling relationships for eight spatial scales between land-use and land cover with respect to LST for Indianapolis, U.S.A., with several landscape metrics commonly used in landscape ecology. In their study of the Baltimore Long Term Ecological Research (LTER) site, Zhou et al. (2011) used fine resolution data and object-based methods to demonstrate that configuration of land cover patches has a significant influence on urban LST. Lastly, Li et al. (2012) revealed a relationship between spatial configuration of green spaces in Beijing, China, with urban LST, as (i) increasing patch density resulting in significantly higher LST when urban greenspace size is unaffected and; (ii) spatial configuration having a significant influence in the variability of derived urban LST.

One key geographical omission from the papers hitherto reviewed are in cities within arid climates, which are amongst the fastest growing in population size and where urbanization rates are projected to remain high (Baker et al. 2004). To this end, we thus investigate the influence of land architectures (Turner in press) on urban LST in the arid city of Phoenix, Arizona in this paper. Our specific objectives are to examine how (i) spatial variation in micro-scale composition of land cover patches, and (ii) the configuration or spatial arrangement of these covers through patch shape and size affect LST. We use fine spatial resolution (2.4 m) remote sensing imagery to characterize land cover patterns within the study area, and we also quantitatively investigate the relationships between landscape pattern and LST through multivariate linear modeling. Improved understanding of the effects of spatial patterns on LST can support land use planning and support development of environmental models. In the arid Southwest U.S.A., where temperatures are already high (frequently reaching over 38 °C in Phoenix) and water resources are sparse, this information can support decisions about urban design and town planning that affect human wellbeing, energy use, and water use.

Study area

Our study area is the Phoenix Metropolitan Area, located in the arid American Southwest at the northern extent of the Sonoran Desert, which extends south into Mexico. Our study is confined to geographic extent of the City of Phoenix (center at 33°24′20″N, 112°5′17″W), which has an area of ~1,340 km^2. Our study area falls within the Central Arizona Phoenix—Long Term Ecological Research (CAP-LTER) study site, which has been the subject of extensive urban ecology studies (Grimm and Redman 2004) and is part of a larger network of ongoing environmental research. Phoenix resides in a valley at ~340 m above sea level. This region receives <180 mm of annual precipitation and experiences mean summer

temperatures of 30.8 °C, although maximum temperatures in July regularly exceed 43.8 °C. Extensive water reclamation projects and large groundwater reserves allowed the valley to develop into an important agricultural region. While agriculture continues to be a major land use in surrounding areas, most agricultural lands in Phoenix have been converted to residential developments, supporting rapid urbanization (Redman and Kinzig 2008).

This expansion into agricultural and desert lands has led Phoenix to become the nation's sixth largest city and one of the most rapidly growing cities in the nation, increasing by ~29 % between 2000 and 2010 to over four million people (Knowles-Yanez et al. 1999; U.S. Census Bureau 2010). Ongoing population growth and urbanization in this region are also associated with increased outdoor water use, which threatens the sustainability of groundwater extraction (Gober et al. 2011). There is a growing shift toward desert landscaping (e.g. Palo Verde/Mesquite trees) in residential areas, but many areas maintain non-native vegetation that demand more water (e.g. Bermuda/Rye grasses and broad-leafed trees). The term xeric landscaping is used to refer to the former style of landscaping and mesic landscaping refers to the ladder. These different types of landscaping are generally clustered into homogenous neighborhoods throughout the city. Mesic areas tend to be in the historic residential areas closer to central Phoenix, where residents have grandfathered water rights. More recent restrictions on water use in new developments have limited outdoor use and encouraged xeric development, as the city has grown outward. In reality the distinction between these classes is sometimes unclear, but we used an a priori classification, in which land cover characteristics distinguish these types.

Though much recent development in Central Arizona took place on retired agricultural lands with historic water rights, a large portion also occurred over previously undeveloped desert lands (Wu et al. 2011), which has resulted in an expanding canopy-layer UHI noticeable at the margins of the greater metropolitan area (Brazel et al. 2007; Georgescu et al. 2009). Recent research by Buyantuyev and Wu (2010) on the surface UHI has shown that the magnitude of intra-urban LSTs, which are strongly affected by non-native vegetation, can be equal to, or even larger than differences between the larger-scale urban core and "rural" (i.e. desert) LST in metropolitan Phoenix. They also suggest that instead of a monolithic "island" of higher urban LSTs, a more appropriate term to describe the intra-urban spatial complexity would be a UHI "archipelago", with multiple hot/cool spots scattered throughout the city. Thus, micro-scale analysis of the spatial composition and configuration of urban LSTs should yield several important insights into this aspect of the Phoenix UHI.

Data and methods

To explore the effects of configuration on LST the following steps were taken: (1) pre-existing land cover and land use maps were incorporated within a geographic information system (GIS), (2) LST was derived from thermal night time satellite image, (3) a selection of landscape metrics were calculated to provide information about land cover configuration, and (4) statistical analysis, specifically Pearson's correlation, analysis of variance, and multiple linear regression, was applied to assess the relationship between LST and the landscape metrics. The following sections provide specific details about these methods.

Land cover data

Land cover and land use differ in that land cover refers to the specific physical materials on the Earth's surface, whereas land use describes the specific human endeavors of an area of land. We used a recently completed fine spatial resolution land cover map for the City of Phoenix. Land cover data were derived from Quickbird imagery obtained in June 2009. The Quickbird imagery has a spatial resolution of 2.4 m and contains four bands (Red, Green, Blue, and Near Infrared). The classified images cover the extent of the City of Phoenix, which has an area of ~1,300 km^2. Scientists classified the Quickbird image using object-based methods in the eCognition software package. Overall accuracy for the classified image was >89 % based on a stratified random sample of validation points. Extensive manual editing corrected for errors in classification and to improve object delineation. The final classified image includes seven land cover types: buildings, grass, trees, soil, impervious surfaces, water, and pools. Natural water features are rare in our study area, but pools are common. Pools were

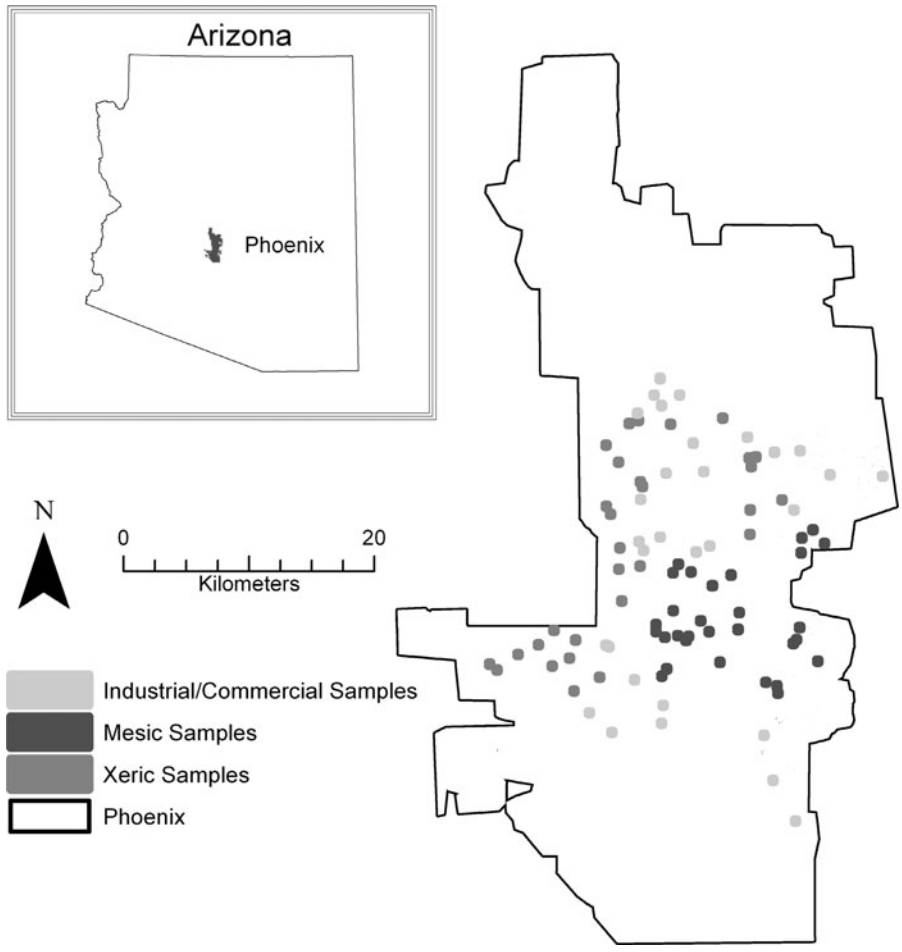

Fig. 1 Locations of randomly selected sampled polygons

distinguished from other water bodies based on their characteristic elliptical and rectilinear shape, as well as their bright aqua-colored liners.

Given the size of the study area and the resolution of the data, we chose to examine a sample set of locations from Quickbird-derived land cover map. We first extracted a subset of urban land uses (xeric and mesic residential, and industrial/commercial) from an existing land use map of the CAP-LTER study area, inclusive of the City of Phoenix (Stefanov et al. 2001, see Redman et al. 2005 for complete land use map used in this study), then used the resulting map to subset our land cover map. The resulting land cover map contained only those locations that were classified as mesic, xeric, or industrial/commercial in Stefanov et al.'s land use map (Fig. 1). Using the ArcGIS software package, we selected thirty random points within each of these three land uses in the city, and created a square buffer (240 × 240 m) around each point (Fig. 1). The points are mainly located in the central area of the city, as a large park areas occupies the majority of Southern Phoenix and the Northern portion of the city remains largely undeveloped. The buffer size of 240 m was selected to be small enough to capture micro-scale LSTs for a cohesive land use category, and to facilitate subsequent comparison to Landsat data at 30 m resolution—hence necessitating a buffer size that is a multiple of 30. Visual inspection ensured that all sampled polygons were properly classified and representative of the land use category. Points that did not appear to be the specified urban land use were discarded and replaced with a new random point. We distinguish between mesic and xeric landscaping because we assume that differences in water use will affect the latent heat flux. As such, we wished to avoid convoluting these effects with differences in structure (Fig. 2).

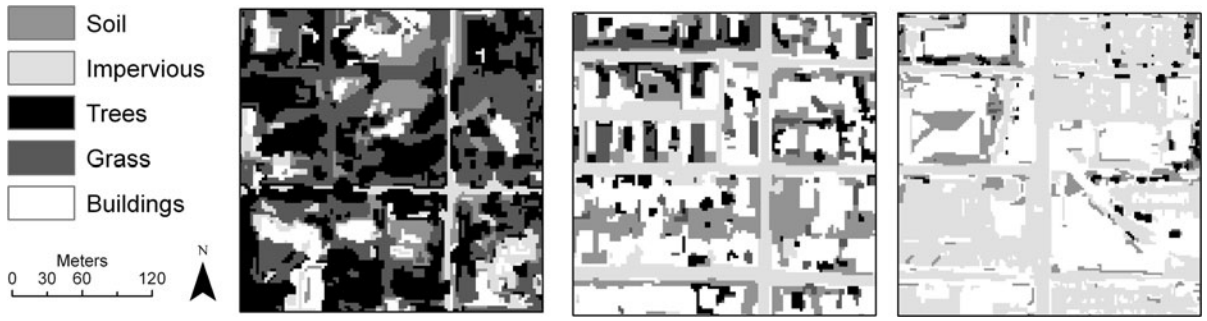

Fig. 2 Land cover for different land uses, mesic residential (*left*), xeric residential (*center*), commercial/industrial (*right*)

Land surface temperature

Given the preponderance of distinct nocturnal UHI phenomena in this city, we analyzed nighttime LSTs in Phoenix in this study. We thus obtained temperature data from an ASTER level-3 product (90-m spatial resolution), which was derived from five bands of thermal infrared data acquired on June 11, 2008, at 2235 h local time (Fig. 3). ASTER Level-3 products apply an algorithm for temperature and emissivity separation (TES). The TES algorithm uses the image's spectral contrast to derive a temperature value with an error of 1.5 °C (Gillespie et al. 1998). In order to estimate mean LST for each sampled polygon, we calculated the value of all ASTER pixels whose centers were within a given sampled polygon. A single mean temperature was assigned to each sampled polygon. The 240 m width of the sampled polygons ensured that multiple temperature points would intersect each plot, and the number of intersecting points varied between four and nine.

Landscape metrics

For all of the sampled polygons, we calculated several landscape metrics using the FRAGSTATS software package (McGarigal and Marks 1995), at both the class-level and landscape-level for each sampled polygon (Table 1). Given our interest in micro-scale differences in landscape, we chose metrics that characterized differences in edge, density of patches, and landscape diversity. We chose six landscape-level pattern metrics (PD, ED, LSI, FRAC_AM, CONTAG, and SHDI) to characterize the overall structure of each sample polygon and five class-level metrics (PLAND, PD, ED, LSI, FRAC_AM) to capture characteristics of specific land covers (see Table 1 for details on each metric). For the class-level metrics, we considered only the classes of grass, buildings, and other impervious surfaces because of their particular relevance to UHI effects and presence in all relevant land uses. Grass, for instance, is known to play an important role in mitigating the UHI by increasing surface latent heat fluxes through evapotranspiration, and is pervasive in mesic residential areas. Trees were uncommon in our

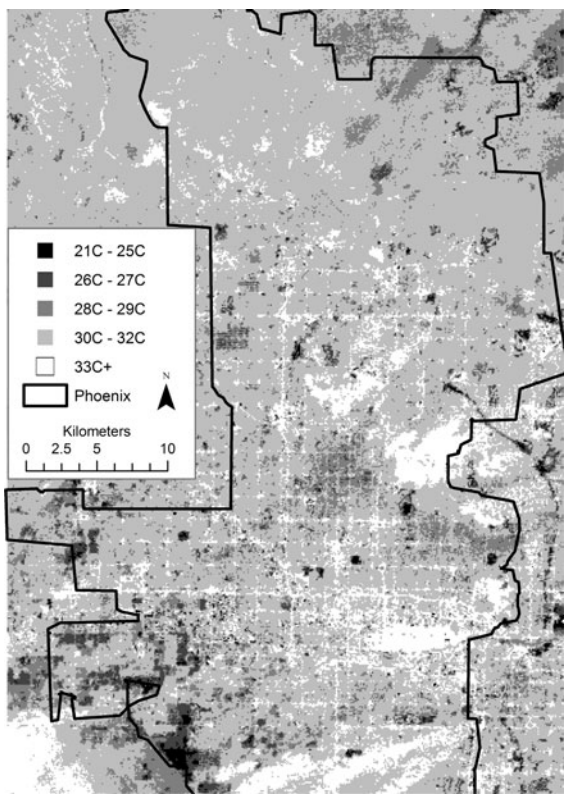

Fig. 3 Image of LSTs within the study area from ASTER taken at 2235 h LT, June 11 2008

Table 1 List of landscape metrics used in this study

Abbreviati on	Metric	Description	Level
PLAND	Percent landscape	The proportion of the total plot occupied by a given and cover class (percent)	Class
PD	Patch density	The number of patches per hectare (Number per hectare)	Class, landscape
ED	Edge density	The sum of the length of all patch edges divided by the total area of the landscape (meters per hectare)	Class, landscape
LSI	Landscape shape index	The total length of edge divided by the shortest possible edge length for the area of a patch (None)	Class, landscape
NP	Number of Patches	A count of the total number of patches (count)	Class, landscape
CA	Class area	The total area of a given class in the entire landscape (hectares)	Class, landscape
TE	Total edge	The length of all edge segments in the landscape (meters)	Class, landscape
FRAC_AM	Fractal dimension	A measure of departure from Euclidean geometry (none)	Class, landscape
CONTAG	Contagion	A measure of the adjacency of patches (percent)	Landscape
SHDI	Shannon's diversity index	A measure of the diversity of land covers (none)	Landscape

random samples for xeric and industrial/commercial land uses, so we excluded these from our analysis.

Statistical analysis

We first used a one-way analysis of variance (ANOVA) to see if the landscape metrics varied among the three land uses. In order to identify specifically which means were different, we used a post hoc least significant difference (LSD) test ($\alpha = 0.05$). Next, we calculated the Pearson's product-moment correlation coefficient to assess the relationship between LST and each of the landscape metrics.

Finally, we created several models of LST using an ordinary least squares (OLS) regression. The dependent variable in our analysis was mean LST for each sampled polygon on the night of June 11, 2008. The independent variables in our analysis were the class level and landscape level metrics listed in Table 1. Based on a priori knowledge, we hypothesized that large differences in water use and different building materials among the land uses would affect the underlying climate LST-regulating process. As such, we created a different set of models for each of the land use types, i.e. mesic, xeric, industrial/commercial. For each land use type, we created multiple models by hand selecting variables that were significantly correlated to LST. We then fit OLS regression models using only these hand-selected variables. For each land use type we also specified a model (models 2, 7, and 10) using a forward selection in SPSS to identify independent variables from the entire set of class and landscape metrics.

To determine if spatial autocorrelation was problematic in our dataset, we used the Lagrange multiplier tests in the Geoda software package (Anselin 2003). This method tests the alternative spatial lag and spatial error models. If the results are significant, then the alternative models should be used. These tests did not indicate any spatial autocorrelation in our data set, thus no further steps were taken to account for spatial dependence.

Results

The analysis of variance on the landscape metrics revealed that the three land uses differed significantly from each other (Table 2) for the majority of landscape-level and class-level metrics. Landscape-level patch density (PD), edge density (ED), landscape shape index (LSI), contagion (CONTAG), and Shannon's diversity index (SHDI), all differed significantly. Only area weighted fractal dimension (FRAC_AM) did not differ significantly among the classes at the landscape-level. In all cases where the *F* value for the ANOVA were significant, the post hoc test indicated that impervious/commercial areas differed from both residential categories, but xeric and mesic areas were not significantly different from each

Table 2 Mean class metrics, as derived from FRAGSTATS, for sampled polygons in three different land uses

Metric	Mesic	Xeric	Industrial	ANOVA
Buildings				
PLAND	17.00	26.71	34.97	17.63**
PD	1333.33	1228.59	622.12	27.03**
ED	738.61	896.40	588.56	9.36**
LSI	10.92	10.87	6.76	31.80**
FRAC_AM	1.17	1.18	1.18	0.13
Impervious				
PLAND	15.24	18.43	37.38	50.96**
PD	767.94	524.89	264.47	12.35**
ED	384.58	506.33	622.44	2.92*
LSI	8.49	7.47	10.56	5.55*
FRAC_AM	1.30	1.31	1.31	0.62
Grass				
PLAND	20.97	13.89	3.96	30.14**
PD	1138.89	1519.68	419.56	55.04**
ED	820.35	711.67	165.04	55.82**
LSI	11.25	11.70	5.49	55.67**
FRAC_AM	1.25	1.19	1.16	20.57**
Landscape				
PD	5839.70	5581.02	2891.25	36.53**
ED	1877.00	1913.71	1155.48	71.91**
LSI	12.86	12.48	7.93	71.91**
FRAC_AM	1.26	1.26	1.25	1.02
CONTAG	34.47	35.92	49.50	50.00**
SHDI	1.53	1.49	1.21	60.47**

See Table 1 for descriptions of metrics

$n = 90$ for Landscape, $n = 30$ for buildings, impervious, and grass

$^{**}p < 0.001$

$^{*}p < 0.01$

other. For nearly all landscape-level metrics (excluding the FRAC_AM), the commercial/industrial sites had lower values than the residential sites. The exception was the CONTAG, which had higher values for the commercial/industrial category.

Similarly, the majority of class-level metrics were significantly different among the land uses. The only landscape metrics that were not significantly different among the categories were the ED of impervious, the area-weighted (FRAC_AM) mean fractal dimension of impervious, and the area-weighted fractal dimension of buildings. The post hoc test indicated that for all other class-level metrics (excluding the aforementioned), except the LSI of impervious, the mean class-level metrics were significantly different between commercial/industrial areas and the residential areas. The PD of all land use classes was lower in commercial/industrial sites than in residential sites. All of the other class-level metrics for buildings and impervious were higher for the commercial/industrial sites, while all of the class-level metrics for grass were significantly lower for the commercial/industrial category. Between the residential categories, mesic and xeric, the means of six class-level metrics were not significantly different: PD of buildings, LSI of buildings, proportion landscape (PLAND) of impervious, ED of impervious, ED of grass, and LSI of grass. Table 2 provides detailed results of the ANOVA.

The results of the ANOVA also show significant differences in mean LSTs among all land uses (Table 2). Mesic residential and xeric residential areas had mean LSTs of 30.18 and 30 °C respectively, and industrial/commercial samples had the highest mean LST, 31.46 °C. Industrial/commercial samples also showed a greater variation of LST across sampled polygons; the standard deviation for LST in industrial/commercial areas was 1.56 °C. In contrast, xeric areas had the smallest standard deviation, 0.52 °C, followed by mesic areas with a slightly larger standard deviation of 0.99 °C.

The Pearson correlation coefficients indicate that the observed relationship between LST and the landscape metrics differed among the three land uses (Table 3). For the xeric sampled polygons, there was not a significant relationship between LST and any of the class-level or landscape-level metrics. In mesic areas, there was a strong positive relationship between LST and the PLAND of buildings ($r^2 = 0.42$, $p = 0.02$) and a strong negative relationship ($r^2 = -0.63$, $p < 0.01$) between the PLAND of grass and LST. For mesic areas, class-level metrics for buildings were the only other metrics that displayed a significant relationship with LST—PD of buildings ($r^2 = 0.48$, $p < 0.01$), ED of buildings ($r^2 = 0.43$, $p < 0.01$), and LSI of buildings ($r^2 = 0.40$, $p < 0.05$). None of the landscape-level metrics were significantly correlated to LST for the residential land uses.

In industrial/commercial areas, several landscape metrics displayed significant relationships to LST. Among the landscape-level metrics, ED, PD, LSI), and area-weighted fractal dimension (FRAC_AM) were all significantly positively correlated to LST. All of the class-level metrics for impervious, except PD were

Table 3 Pearson's correlation coefficients between class metrics and LST

Metric	Mesic	Xeric	Industrial
Buildings			
PLAND	0.42**	0.06	−0.56**
PD	0.48**	−0.10	0.32†
ED	0.43**	0.01	−0.05
LSI	0.40*	−0.04	0.21
FRAC AM	0.06	0.17	−0.29
Impervious			
PLAND	−0.03	−0.15	0.55**
PD	−0.06	0.26	0.06
ED	−0.04	−0.05	0.64**
LSI	−0.07	0.04	0.44*
FRAC_AM	0.10	−0.31†	0.48**
Grass			
PLAND	−0.63**	0.15	−0.20
PD	0.07	−0.01	0.14
ED	−0.28	0.05	0.13
LSI	0.10	−0.02	0.21
FRAC AM	−0.24	0.18	0.19
Landscape			
ED	0.34†	0.12	0.45*
PD	0.29	0.13	0.37*
LSI	0.34†	0.12	0.45*
SHDI	0.10	0.15	0.27
CONTAG	−0.28	−0.28	−0.30
FRAC_AM	0.20	−0.12	0.45*

See Table 1 for description of metrics

$n = 90$ for Landscape, $n = 30$ for buildings, impervious, and grass

* $p < 0.05$

** $p < 0.01$

† $p < 0.1$

strongly positively correlated to LST. In addition, the PLAND of buildings was strongly negatively correlated to temperature ($r^2 = -0.56$, $p < 0.01$).

The regression results offer insights into the influence of spatial configuration on LST in Phoenix. Models 1 and 2 used LST for all sampled polygons, including mesic, xeric and industrial/commercial land uses, and the dependent variable (Table 4). Model 2, derived with forward selection, provides the best estimate of LST for all sites. This model explained ~34 % of the variation in LST. Proportion landscape of impervious (Imp_PLAND) and proportion landscape of grass (Grass_PLAND) were the only two variables selected. A 1 % increase in impervious area increased temperature by 0.32°, whereas a 1 % increase in grass decreased temperatures by 0.34°.

When the data were split into three categories, the models better explained the variation in temperatures. Model 7 was the best model for the industrial/commercial land use category. This model explained ~62 % of the variation in LST in the industrial/commercial sites. Increases in the ED of impervious cover and fractal dimension of grass cover both resulted in higher LST for the industrial/commercial category. Increases in the PD of impervious cover decreased LST. Model 10 produced the best results for estimating LST in the mesic land use category. This model explained about 40 % of the variation in LST. Although models 8, 9, and 10 had identical r^2 values, the adjusted r^2 was highest for Model 10, indicating that the additional variables in the prior models did not improve the fit of the models. For model 10, increases in proportion landscape of grass (grass_PLAND) and impervious (imp_PLAND) both decreased LST. Our model specification for xeric land use failed to generate any significant results.

Discussion

Many of the results from this analysis were expected given the known relationships between land cover and LST. There were, however, several findings that we found surprising and believe merit further discussion. In the remainder of the paper, we discuss these findings, consider the implications of these results, and suggest several places for future inquiry.

Initial analysis of variance and descriptive statistics revealed the anticipated relationship between LST and land use, with increasingly high temperatures in the mesic, xeric, and commercial/industrial land uses. The higher standard deviation for LST in industrial/commercial areas may help to explain why the subsequent analyses were able to better explain the variation in temperatures. Unexpectedly, all of the measures of area-weighted mean fractal dimension (FRAC_AM) were quite similar among all of the land uses. All of the land uses appear to have relatively low degrees of edge complexity for patches of different cover types.

The Pearson's correlation coefficients provided some of the more surprising results of this analysis

Table 4 Results from the linear regression models

Land use	Model	Variables	Coefficient	Stand. Coeff.	Model R^2	Adjusted R^2
All	1	Imp_PLAND	0.29*	0.31	0.27	0.26
		Grass_PLAND	−0.50*	−0.45		
		Build_PLAND	−0.23*	−0.26		
All	2	Imp_PLAND	0.33**	0.36	0.34	0.32
		Grass_PLAND	−0.34**	−0.31		
Industrial/ Commercial	3	Build_PLAND	−0.40*	−0.44	0.42	0.35
		Imp_PLAND	0.28	0.25		
		Grass_PLAND	−0.56	−0.19		
Industrial/ commercial	4	Imp_PLAND	0.68**	0.61	0.44	0.40
		L_SHDI	31.76**	0.37		
Industrial/ commercial	5	Imp_PLAND	0.58**	0.52	0.48	0.44
		L_LSI	3.50**	0.42		
Industrial/ commercial	6	Imp_ED	0.04**	0.51	0.54	0.50
		Build_PLAND	−0.34*	−0.38		
Industrial/ commercial	7	Imperv_ED	0.07**	0.93	0.62	0.58
		Imperv_PD	−0.05**	−0.50		
		Grass_FRAC	73.94*	0.27		
Mesic	8	Build_PLAND	−0.18	−0.09	0.40	0.33
		Imp_PLAND	−0.48	−0.61		
		Grass_PLAND	0.05*	0.04		
Mesic	9	Imp_PLAND	−0.14	−0.99	0.40	0.33
		Grass_PLAND	−0.45**	−0.57		
		Build_ED	−0.003	0.11		
Mesic	10	Imp_PLAND	−0.16	−0.83	0.40	0.36
		Grass_PLAND	−0.50**	−0.67		

For all models, LST is the dependent variable

$n = 90$ for Landscape, $n = 30$ for buildings, impervious, and grass

$^{**}p < 0.01$

$^{*}p < 0.05$

(Table 3). While we assume that proportion of landscape (PLAND) would be similarly correlated to LST for all cover types and in all land uses, the results show that the relationship between LST and specific cover types varies with the different land uses. Most notably, none of the metrics, including PLAND were correlated to LST for xeric areas. While it is possible that other cover types, particularly soil, may reveal a relationship to LST, the overall landscape-level metrics also failed to show any significant relationship to LST. Most likely, the lack of relationship is due to a lack of variation in LST among the xeric land use sites (standard deviation of LST was 0.51 °C). Given that proportional area of grass explains much of the variation in mesic temperatures, the low levels of grass in xeric areas could account for lower variance in LST.

The relationship between the proportional area of buildings is generally assumed to be positively correlated to LST. Although this was true for Mesic land uses, our results reveal a significant strong negative relationship in industrial/commercial sites. A combination of three factors is likely to explain this relationship. First, given the strong positive relationship between impervious surfaces, which dominate industrial/commercial sites, any additional building space will likely result in a reduction of impervious space, thus lowering temperatures. Second, industrial/commercial buildings tend to be larger structures in this area and therefore may offer shading for a portion of the day. Third, many industrial/commercial building in Phoenix have been constructed with white roofs to increase albedo.

The results of the OLS regression models indicate that proportional area of grass and impervious cover best explain variation in LST for the mesic land use category and for all sites collectively. In contrast, the measures of configuration, impervious ED,

impervious PD, and fractal dimension of grass cover, best explain changes in LST for commercial/industrial sites. These results indicate that the degree of edge complexity and the patchiness of cover types may affect LST for this land use category. Interestingly, an increase in the fractal dimension of grass led to an increase LST. This result suggests that less complex shapes of grass patches may better regulate LST. Increases in PD of impervious cover lowered LST. Higher PD in industrial/commercial settings likely indicated more intervening features of grass, trees, or buildings, which likely alter the heat flux through their interactions.

In order to fully evaluate the tradeoffs in environmental amenities that result from management and design policy, decision-makers should consider the consequences of landscape structure for multiple processes. Urbanization within the CAP-LTER study area has increased spatial complexity through greater heterogeneity of land covers and fragmentation of natural land covers (Wu et al. 2011), with varying degrees of spatial complexity in different areas of the city (York et al. 2011). While this change in spatial structure has been well documented, as well as its impact on urban temperatures (e.g. Brazel et al. 2000; Buyantuyev and Wu 2010), it remains unclear what the implications are for many biophysical processes. The relationship between spatial structure and other ecosystem services requires further investigation in this rapidly changing environment, particularly if decision-makers are to actively manage the configuration of the urban mosaic. Optimizing the configuration of the landscape to reduce the detrimental impacts of the larger-scale UHI may allow land managers to more effectively balance the tradeoffs between water, energy, and temperature in this arid region. Further research is needed, but it appears that creating more complex landscapes, with more building edges and complex shapes of grass patches may contribute to lower micro-scale LST in industrial/commercial areas and possibly in mesic residential areas. This action potentially increases small-scale thermal comfort while implying reduced irrigation water use in this desert city.

Limitations

Several factors may influence our results and should be included in future analysis. First, we did not consider the full array of variables that influence UHI, including building materials and local climatic conditions. It is likely that the building materials varied across our sampled polygons, and these differences are not represented in our land cover typology. Furthermore, the topography surrounding the various sites also influences temperature, and we did not control for variation in topography among sites. As our results were based on temperatures for a single night, additional analysis should examine multiple dates and compare daytime temperatures. Lastly, as a major effect of the UHI is a reduced variation between daytime and nighttime temperatures, further research should examine the effects of spatial pattern on daytime temperature ranges.

Accurately measuring surface temperatures can be problematic in urban environments where emissivity varies among heterogeneous building materials (Becker 1987). The TES algorithm used by ASTER Level 3 temperature products provides consistently accurate LST measurements when emissivity values of materials are fairly high (Gillespie et al. 1998), but errors may occur when materials in the built environment are made of polished metal, which often has a low emissivity value. In general, these low emissivity materials are only of concern when they are a dominant land cover. ASTER temperatures are averaged over a 90 m pixel, which reduces the impact of low emissivity materials that comprise only a small amount of the pixel.

Finally, in our analysis, we did not control for composition when testing configuration variables because we wanted to test for the effects of composition also. Our results for the effects of configuration would likely be altered if we had controlled our samples by choosing sites that had similar compositions of land covers. Future analysis should build on this analysis by controlling for composition and testing additional configuration variables.

Conclusions

Alteration of land cover composition has been established as a driver of local climate change (Quattrochi and Ridd 1994). The resulting effects of the UHI have implications for human health and biophysical processes. The research presented here corroborates previous findings regarding the implications of land cover for

LST, but also indicates that the relative impacts of land cover on LST vary among land uses. The interplay of multiple variables that influence temperature will differ among these categories, thus altering the importance of land cover for mitigating the effects of the UHI. For example, in industrial/commercial areas, which are predominantly covered by buildings and impervious surfaces, the presence of buildings is correlated to lower temperatures. In contrast buildings are positively correlated to temperature in mesic residential areas. These results also indicate that landscape composition influences temperature, but this relationship is not consistent for all areas and land uses. Context plays an important role in determining the impact of land cover on temperature. As with composition, the impacts of configuration are context-dependent, and no single configuration variable explained variability for all land uses in this study. In those examples where spatial configuration explains LST, edge characteristics (e.g. fractal dimensions and ED) are particularly important. For industrial/commercial areas in particular, ED appears particularly important for explaining variations in LST. The findings have important implications for land use planning and urban design. In order to reduce UHI effects, planners must consider the composition and configuration of the landscape. In addition, they must carefully consider context and the interplay of land covers. These results should inform future study of UHI effects, particularly for improving existing models. Future work should expand this research to consider more land uses in different environments and for different times.

Acknowledgments We thank B. L. Turner II and Anthony Brazel for comments, and Shai Kaplan for his work on classifying the Quickbird image. This work was supported by the National Science Foundation under grant no. BCS-1026865 (CAP-LTER) and the Gilbert F. White Professorship, and was carried out in the Environmental Remote Sensing and Geoinformatics Lab of the Global Institute of Sustainability and the School of Geographical Science and Urban Planning, ASU. WTLC's research is funded by a NSF Earth Systems Models (EaSM) Program award 1049251.

References

Anselin L (2003) Geoda 0.9 User's Handbook

Baker LA, Brazel AJ, Westerhoff P (2004) Environmental consequences of rapid urbanization in warm, arid lands: case study of Phoenix, Arizona (USA). In: Marchettini N, Brebbia C, Tiezzi E, Wadhwa LC (eds) The sustainable city III, (Proceedings of the Sienna Conference, held June 2004), Advances in Architecture Series, WIT Press, Boston

Becker F (1987) The impact of spectral emissivity on the measurement of land surface temperature from a satellite. Int J Remote Sens 8:1509–1522

Brazel A, Selover N, Vose R, Heisler G (2000) The tale of two climates—Baltimore and Phoenix urban LTER sites. Climate Res 15:123–135

Brazel A, Gober P, Lee S-J, Grossman-Clarke S, Zehnder J, Hedquist B, Comparri E (2007) Determinants of changes in the regional urban heat island in metropolitan Phoenix (Arizona, USA) between 1990 and 2004. Climate Res 33:171–182

Buyantuyev A, Wu J (2010) Urban heat islands and landscape heterogeneity: linking spatiotemporal variations in surface temperatures to land-cover and socioeconomic patterns. Landscape Ecol 25(1):17–33

Cao X, Onishi A, Chen J, Imura H (2010) Quantifying the cool island intensity of urban parks using ASTER and IKONOS data. Landsc Urban Plan 96:224–231

Chow WTL, Chuang WC, Gober P (2012) Vulnerability to extreme heat in metropolitan Phoenix: spatial, temporal, and demographic dimensions. Prof Geogr 64:286–302

Georgescu M, Miguez-Macho G, Steyaert LT, Weaver CP (2009) Climatic effects of 30 years of landscape change over the greater Phoenix, Arizona, region: 1. Surface energy budget changes. J Geophys Res 114:D05110

Gillespie A, Rokugawa S, Matsunaga T, Cothern JS, Hook S, Kahle AB (1998) A temperature and emissivity separation algorithm for advanced spaceborne thermal emission and reflection radiometer (ASTER) images. IEEE T Geosci Remote 36:1113–1126

Gober P (2006) Metropolitan Phoenix: place making and community building in the desert. University of Pennsylvania, Philadelphia

Gober P, Wentz EA, Lant T, Tschudi MK, Kirkwood CW (2011) WaterSim: a simulation model for urban water planning in Phoenix, Arizona, USA. Environ Plann B 38:197–215

Goward SN, Cruickshanks GD, Hope AS (1985) Observed relation between thermal emission and reflected spectral radiance of a complex vegetated landscape. Remote Sens Environ 18:137–146

Grimm NB, Redman CL (2004) Approaches to the study of urban ecosystems: the case of central Arizona–Phoenix. Urb Ecosyst 7:199–213

Gustafson EJ (1998) Quantifying landscape spatial pattern: what is the state of the art? Ecosystems 1:143–156

Harlan SL, Brazel A, Prashad L, Stefanov W, Larsen L (2006) Neighborhood microclimates and vulnerability to heat stress. Soc Sci Med 63:2847–2863

Jenerette GD, Harlan SL, Brazel A, Jones N, Larsen L, Stefanov WL (2007) Regional relationships between surface temperature, vegetation, and human settlement in a rapidly urbanizing ecosystem. Landscape Ecol 22:353–365

Jin MS (2012) Developing an index to measure urban heat island effect using satellite land skin temperature and land cover observation. J Clim 25:6193–6201

Kalkstein LS, Smoyer KE (1993) Human biometeorology—the impact of climate-change on human health—some international implications. Experientia 49:969–979

Kalnay E, Cai M (2003) Impact of urbanization and land-use on climate. Nature 423:528–531

Kinney P, Shindell D, Chae E (2001) Climate change and public health: impact assessment for the NYC metropolitan region. In: Rosenzweig C, Solecki WD (eds) Climate change and a global city: an assessment of the metropolitan east coast region. Columbia Earth Institute, New York

Klinenberg E (2002) Heat wave: a social autopsy of disaster in Chicago. University of Chicago Press, Chicago

Knowles-Yanez K, Moritz C, Fry J, Redman CL, Bucchin M, McCartney PH (1999) Historic land use: phase I report on generalized land use. Central Arizona-Phoenix Long-Term Ecological Research. Arizona State University, Tempe

Landsberg HE (1981) The urban climate. National Academy Press, New York

Lee S-M, Fernando HJS, Princevac M, Zajic D, Sinesi M, McCulley JL, Anderson J (2003) Transport and diffusion of ozone in the nocturnal and morning planetary boundary layer of the Phoenix valley. Environ Fluid Mech 3:331–362

Li X, Zhou W, Ouyang Z, Xu W, Zheng H (2012) Spatial pattern of greenspace affects land surface temperature: evidence from the heavily urbanized Beijing metropolitan area, China. Landscape Ecol 27:887–898

Liu H, Weng Q (2009) Scaling effect on the relationship between landscape pattern and land surface temperature: a case study of Indianapolis, United States. Photogramm Eng Remote Sens 75(3):291–304

McGarigal K, Marks BJ (1995) FRAGSTATS: spatial pattern analysis program for quantifying landscape structure. General Technical Report PNW-GTR-351. Pacific Northwest Research Station, USDA-Forest Service, Portland

Nichol JE (1996) Fine resolution surface temperature patterns related to urban morphology in a tropical city: a satellite-based study. J Appl Meteorol 35:135–152

Oke TR (1987) Boundary layer climates, 2nd edn. Routledge, London

Oke TR (1995) The heat island of the urban boundary layer: characteristics, causes and effects. In: Cermak JE (ed) Wind climate in cities. Kluwer Academic Publishers, Netherlands

Oke TR (2004) Initial guidance to obtain representative meteorological observations at urban sites. IOM Report 81.TD, World Meteorological Organization, Geneva

Quattrochi DA, Ridd MK (1994) Measurements and analysis of thermal energy responses from discrete urban surfaces using remote sensing data. Int J Remote Sens 15:1991–2002

Quattrochi D, Luvall J, Rickman D, Estes M, Laymon C, Howell B (2000) A decision support information system for urban landscape management using thermal infrared data. Photogramm Eng Rem S 66:1195–1207

Redman CL, Kinzig AP (2008) Water can flow uphill: a narrative of central Arizona. In: Redman CL, Foster D (eds) Agrarian landscapes in transition. Oxford University Press, New York, pp 238–271

Redman CL, Hutchins J, Kunda R (2005) Land use classification 2000. http://caplter.asu.edu/data/. Accessed online August 2011

Rosenzweig C, Solecki W, Parshall L, Chopping M, Pope G, Goldberg R (2005) Characterizing the urban heat island in current and future climates in New Jersey. Global Environ Change B 6:51–62

Small C (2005) A global analysis of urban reflectance. Int J Remote Sens 26:661–681

Stefanov WL, Ramsey MS, Christensen PR (2001) Monitoring urban land cover change: an expert system approach to land cover classification of semiarid to arid urban centers. Remote Sens Environ 77:173–185

Turner BL (2010) Sustainability and forest transitions in the Southern Yucatan: the land architecture approach. Land Use Policy 27:170–179

Turner MG, Gardner RH, O'Neill RV (2001) Landscape ecology in theory and practice. Springer, New York

U.S. Census Bureau (2010) United States Census: 2010. http://2010.census.gov/2010census/. Accessed online 1 July 2011

Voogt JA, Oke TR (2003) Thermal remote sensing of urban climates. Remote Sens Environ 86:370–384

Weng Q (2003) Fractal analysis of satellite-detected urban heat island effect. Photogramm Eng Remote Sens 69(5):555–566

Weng Q, Liu H, Liang B, Lu D (2008) The spatial variations of urban land surface temperatures: pertinent factors, zoning effect, and seasonal variability. IEEE J Sel Top Appl Earth Obs Remote Sens 1(2):154–166

Wu J, Jenerette GD, Buyantuyev A, Redman CL (2011) Quantifying spatiotemporal patterns of urbanization: the case of the two fastest growing metropolitan regions in the United States. Ecol Complex 8:1–8

York AM, Shrestha M, Boone CG, Zhang S, Harrington JA, Prebyl TJ, Swann A, Agar M, Antolin MF, Nolen B, Wright JB, Skaggs R (2011) Land fragmentation under rapid urbanization: a cross-site analysis of Southwestern cities. Urban Ecosyst 14:429–455

Zhang X, Zhong T, Feng X, Wang K (2009) Estimation of the relationship between vegetation patches and urban land surface temperature with remote sensing. Int J Remote Sens 30:2105–2118

Zhou W, Huang G, Cadenasso ML (2011) Does spatial configuration matter? Understanding the effects of land cover pattern on land surface temperature in urban landscapes. Landsc Urban Plan 102:54–63